Article

Activity-based Near-Infrared Fluorogenic Probe Enables In Vitro and In Vivo Profiling of Neutrophil Elastase

Shi-Yu Liu, Hao Xiong, Rong-Rong Li, Wen-Chao Yang, and Guang-Fu Yang

Anal. Chem., **Just Accepted Manuscript** • DOI: 10.1021/acs.analchem.8b04455 • Publication Date (Web): 10 Jan 2019

Activity-based Near-Infrared Fluorogenic Probe Enables *In Vitro* and *In Vivo* Profiling of Neutrophil Elastase

Shi-Yu Liu,[†,§] Hao Xiong,[†,§] Rong-Rong Li,[†] Wen-Chao Yang,[*,†] and Guang-Fu Yang[*,†‡]

[†]Key Laboratory of Pesticide & Chemical Biology of Ministry of Education, International Joint Research Center for Intelligent Biosensor Technology and Health, and Chemical Biology Center, College of Chemistry, Central China Normal University, Wuhan 430079, P.R. China

[‡]Collaborative Innovation Center of Chemical Science and Engineering, Tianjin 30071, P.R. China.

[§] These two authors made equal contributions.

* Wen-Chao Yang, e-mail: tomyang@mail.ccnu.edu.cn; Tel: 86-27-67867706; Fax: 86-27-67867141; Guang-Fu Yang, e-mail: gfyang@mail.ccnu.edu.cn; Tel: 86-27-67867800; Fax: 86-27-67867141.

Abstract

Neutrophil elastase (NE), a typical hematopoietic serine protease, has significant roles in inflammatory and immune responses, and thus highly associated with various diseases such as acute lung injury (ALI) and lung cancer. Rapid and accurate measurement of NE activity in biological systems is particularly important for understanding the role of NE in inflammatory diseases, as well as the clinic diagnosis. However, the specific detection and non-invasive imaging of NE *in vivo* remains a challenge. To address this issue, a small-molecule substrate-based near-infrared fluorogenic probe (**NEP)** for NE was constructed *via* incorporating pentafluoroethyl as the recognition group with a hemicyanine dye-based fluorophore. This initially quenched probe possesses over than 25-fold red fluorescence enhancement upon the catalysis of human NE and the detection limit is about 29.6 ng/mL. In addition, the high specificity and the long emission wavelength (λ_{em}max = 700 nm) of **NEP** allowed the direct monitoring of NE-trafficking, exogenous NE up taking and endogenous NE up-regulation at the cellular level. Moreover, the successfully spatiotemporal imaging of NE in ALI model mice also made it a promising new tool in clinical diagnosis for ALI and other lung diseases.

Keywords

Neutrophil elastase, fluorogenic probe, intracellular trafficking, acute lung injury.

INTRODUCTION

Neutrophils are viewed as critical immune cells in inflammatory response for preventing invasion by micro-organisms and clearance of extracellular pathogens.[1] When neutrophils are recruited to site of inflammation, neutrophil elastase (NE) can promote inflammatory responses in many human diseases.[2] Human NE (EC 3.4.21.37) consisting of 267 amino acid residues[3], is of high proteolytic activity which could resulted in protease-dependent tissue destruction in the inflammatory sites[4] and also is implicated in regulation of cytokine network[4]. Therefore, the activation of human NE and its distribution is highly crucial for the regular and abnormal inflammatory responses.

Extensive studies showed that NE was elevated in various inflammatory diseases especially lung diseases, such as acute lung injury (ALI) and chronic obstructive pulmonary disease (COPD).[5-7] In those diseases, NE was recruited and gathered in lung tissue, and thus caused the tissue damage and endothelial cell injury[8-9] This systemic inflammatory response syndrome induced organ dysfunction further leads to increased permeability, vasodilation, and activation of the coagulation cascade.[10] Thus, human NE is validated as a biomarker of disease progression, and a therapeutic target for drug discovery. Selective inhibition of NE activity was found to be an effective solution for treatment of the above diseases. Sivelestat, the only commercial human NE inhibitor, was reported to significantly prolonged survival in animal model study[6-7] and clinical investigation[10]. However, another clinical trial revealed that ALI patients treated with sivelestat did not associated with decreased mortality[11] and a new generation of NE selective inhibitor, AZD9668, failed in the phase II clinical trial of COPD.[12] The failure of the above therapeutics may be partially attributed to the insufficient understanding of the NE-related pathological mechanism. Besides, NE is also known as an important hallmark of lung cancer[13], which has a critical role in accelerate of lung tumor growth[14] and promotion of tumor invasion and metastasis[3] and even connected with insulin resistance[15]. Thus, developing a tool for spatiotemporal monitoring of NE in living cells and *in vivo* is of great importance,

which would facilitate the thorough and comprehensive understanding of the function of NE in lung diseases.

Small molecule-based fluorescent substrate for protease has aroused great interests over the last two decades. With the high spatial and temporal resolution[16], it is capable of tracing enzymes trafficking of its subcellular location in real-time manner[17-18], studying the related biological function of enzymes[19-20] and monitoring of regulation of protein level in cell level animal disease model *in vivo*[21-22]. Previously, we discovered the first non-peptide-based fluorogenic substrate for elastase. However, the green fluorophore of that probe and its limited specificity impede its application for NE detection and imaging in living organisms. Hence, we herein report the identification of a small molecule-based near-infrared fluorogenic probe (named **NEP**) for human NE and the application in cellular an *in vivo* imaging (Scheme 1). On the basis of the comprehensive characterization, **NEP** displays excellent features for the specific human NE detection in physiologically relevant environment with ~25-fold higher fluorescence enhancement and ~29.6 ng/mL of the detection limit. More importantly, this probe enabled the spatially resolved monitoring of cellular NE-trafficking, exogenous NE uptake and endogenous NE up-regulation. In addition, it could image the elevated NE level in ALI model mice compared to health control. These findings indicate that **NEP** could be a valuable tool to be applied in a definitive diagnosis of ALI and molecule-level pathophysiological investigations of lung diseases.

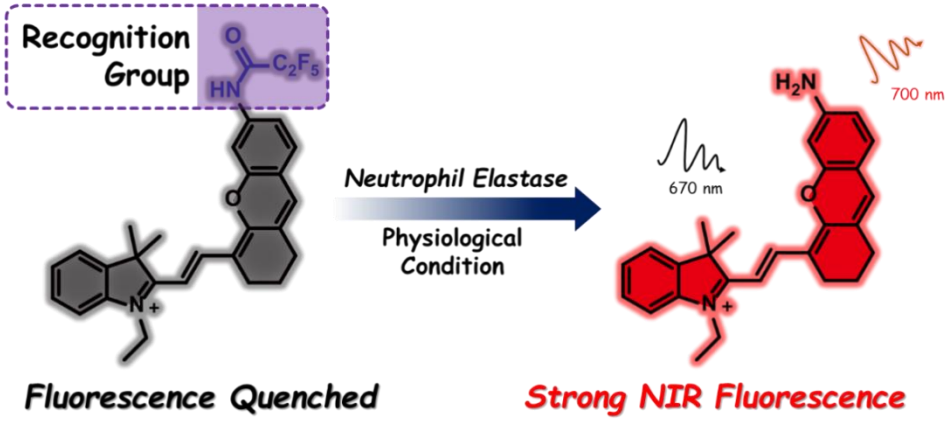

Scheme 1. Sensing mechanism for human NE with designed probe.

EXPERIMENTAL SECTION

Organic synthesis.

Reagents. The reactants used in this article were all commercially available and purchased from regular manufacturers. The solvents used in silica gel column chromatography (CC) were purchased from Chinasun Specialty Products Co., Ltd. and Wuhan Shenshi Chemical & Instrument Co., Ltd. Meanwhile, the silica gel (200-300 mesh) used in chromatography was brought from Qingdao Haiyang Chemical Co., Ltd.

Instrumentation. The cuvette (Hellma, Germany) on the microplate reader (SpectraMax M5, Molecular Devices) was used to measure the UV-Vis absorption spectrum and fluorescence spectrum, while the black 96-well microplate (Corning, America) one the same microplate reader was applied in the inhibitory studies. The structure of key intermediate was characterized through GC-MS (ESI) and ^{1}H NMR (Varian Mercury 400 MHz Plus), while the target compound was identified through HRMS (MALDI; AB SCIEX TOF/TOF ™ 5800 System), ^{1}H/^{13}C NMR (Varian Mercury 400 or 600 MHz Plus), respectively. The fluorescence images were acquired by inverted fluorescence microscope (Olympus IX71, Japan) and the *in vivo* imaging study was carried out with IVIS Lumina XRMS III (PerkinElmer, USA).

The preparation of HCY-NH$_2$ (Scheme 2). The intermediates **I-1**, **I-2**, **Cy7Cl** and **HCY-NH$_2$** were synthesized according to the published procedures.[22-23] The key intermediate **HCY-NH$_2$** (277 mg) was prepared with **Cy7Cl** (639 mg, 1.0 mmol) and 3-nitrophenol (347 mg, 2.5 mmol) as starting materials and purified by column chromatography (DCM/MeOH = 40/1 to 5/1, V/V) with the yield of 52.8%. **^{1}H NMR** (600 MHz, DMSO-d_6) δ 8.45 (d, J = 14.4 Hz, 1H), 7.68 (s, 2H), 7.50 – 7.38 (m, 2H), 7.36 – 7.28 (m, 1H), 6.87 (s, 1H), 6.73 (d, J = 8.6 Hz, 1H), 6.66 (s, 1H), 6.27 (d, J = 14.4 Hz, 1H), 4.27 (s, 2H), 2.69 (d, J = 18.8 Hz, 4H), 1.89 – 1.77 (m, 2H), 1.71 (s, 6H), 1.32 (t, J = 7.2 Hz, 3H). **GC-MS** (ESI) calcd for $[C_{27}H_{29}N_2O]^+$, 397.22; found, 397.54.

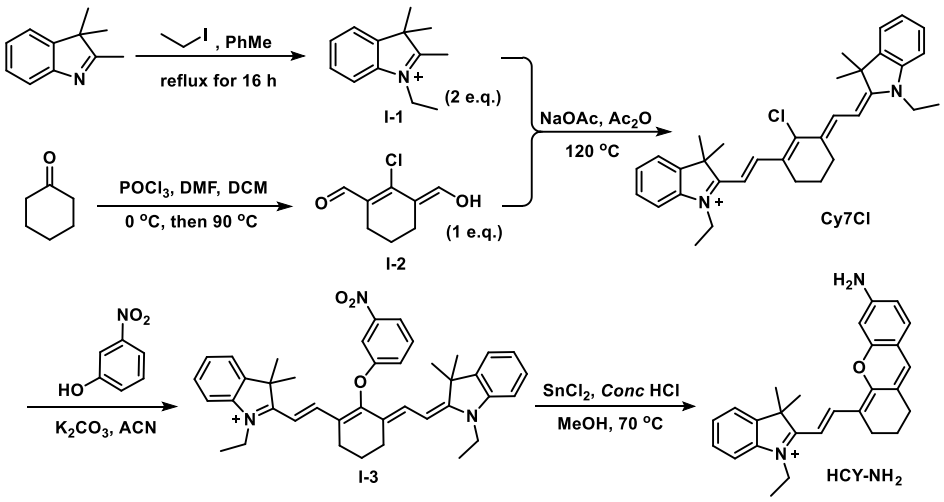

Scheme 2. The synthesis of the intermediates **I-1**, **I-2**, **Cy7Cl, I-3** and **HCY-NH2**.

The synthesis of NEP (Scheme 3). In, **HCY-NH2** (155 mg, 0.3 mmol) was added to the solution of anhydrous dichloromethane, and then triethylamine (606 mg, 0.6 mmol) was added dropwise into the round-bottomed flask by a syringe at room temperature until the reactants were sufficiently dissolved. After a while, the solution of 2,2,3,3,3-pentafluoropropanoic anhydride (CAS ID: 356-42-3; 186 mg, 0.6 mmol) dissolved in the same dichloromethane was added slowly with a dropping funnel in an ice bath. The reaction mixture was stirred for 3 h at room temperature until **HCY-NH2** almost ran out (TLC monitoring). The reaction solution was washed sequentially by H_2O (2 ×) and saturated sodium chloride solution (1×) immediately after the reaction completed. Then the organic layer was dried over anhydrous Na_2SO_4 and concentrated with the rotary evaporator. The combined residue was eventually separated and purified by the silica gel chromatography (DCM/MeOH = 60/1 to 20/1, V/V) to generate a purple solid **NEP** (72 mg) as final product with the yield of 36.4%. **^{1}H NMR** (400 MHz, DMSO-d_6) δ 11.81 (s, 1H), 8.60 (d, J = 15.1 Hz, 1H), 7.91 (d, J = 2.0 Hz, 2H), 7.84 (d, J = 7.4 Hz, 1H), 7.76 (d, J = 8.0 Hz, 1H), 7.68 (dd, J = 8.5, 2.0 Hz, 1H), 7.62 – 7.54 (m, 2H), 7.50 (t, J = 7.4 Hz, 1H), 7.43 (s, 1H), 6.68 (d, J = 15.1 Hz, 1H), 4.50 (q, J = 7.0 Hz, 2H), 3.10 (q, J = 7.4 Hz, 3H), 2.72 (dt, J = 25.4, 6.3 Hz, 4H), 1.87 – 1.81 (m, 2H), 1.77 (s, 6H), 1.40 (t, J = 7.2 Hz, 3H), 1.18 (t, J = 7.2 Hz, 6H). **^{13}C NMR** (150 MHz, DMSO-d_6) δ 177.80, 159.19, 157.92, 155.68, 152.36, 145.37, 142.45, 140.97, 139.05, 131.05, 129.59, 129.06, 128.16,

127.63, 123.00, 119.19, 117.83, 114.28, 113.56, 107.48, 105.70, 50.76, 45.55, 40.64, 28.67, 27.15, 23.56, 19.82, 12.91, 8.53. **HRMS** (MALDI) calcd for $[C_{30}H_{28}F_5N_2O_2]^+$, 543.2065; found, 543.1636.

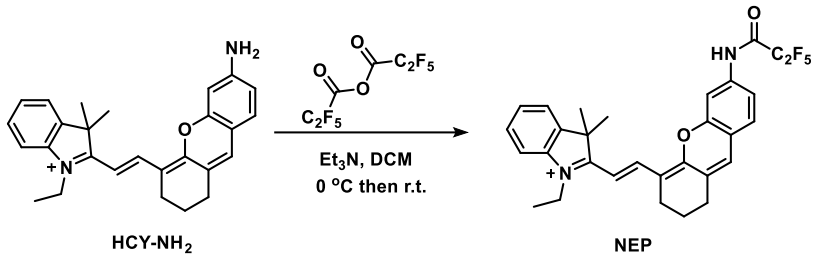

Scheme 3. The synthesis of the target probe **NEP**.

Specific detection of NE in aqueous solution. The sensing capability of **NEP** (10 μM) toward human NE was tested in 10 mM phosphate buffer at different pH and temperature. Under the optimized condition, both the time- and concentration-dependent fluorescence response of **NEP** in the presence of human NE were then measured by fluorescence increasement of the reaction system at the maximum emission wavelength of 700 nm (λ_{ex}max = 670 nm). The specificity study of **NEP** toward NE and other commonly used enzymes (0.01 mg/mL) was also performed by evaluating the final increased fluorescence intensity ($F-F_0$). For the detection of NE activity in mouse serum and broncho-alveolar lavage (BAL), each 100 μL of mouse serum or BAL were pre-incubated with or without 10 μM sivelestat for 10 min, followed by the addition of 10 μM **NEP** for 30 min, the enhanced fluorescence intensity at 700 nm was measured by microplate reader.

Cell culture and cellular imaging. Human non-small cell lung carcinoma cells were grown in 1640 (Gibco, USA) medium supplemented with 10% (V/V) fetal bovine serum (Gibco, USA). Rat basophilic leukemia cell RBL-2H3 cells were grown in MEM (Gibco, USA) medium supplemented with 15% (V/V) heat-activated fetal bovine serum (Gibco, USA). Both cell lines were maintained at 37 °C and 5% CO_2, and were seeded at a density around 3×10^5 cells on a glass-bottom cell culture dishes (NEST, 15 mm) in the day before the experiment. Next day, after washed with PBS

for three times, the cells pre-incubated with 10 μM inhibitors (DHPI or sivelestat) or DMSO for 2 h were treated with **NEP** accordingly. For the NE trafficking experiments, cells were pre-incubated with or without 2 μM Brefeldin A (BFA) for 16 h before cell imaging. Similarly, cells were pre-incubated with lipopolysaccharide (LPS, 20 μg/mL), interleukin 6 (IL-6, 100 ng/mL) or tumor necrosis factor alpha (TNF-α, 100 ng/mL) for 24 h, respectively, and then imaged for the inflammation study. To understand the cellular up-take of human NE, cells were pre-incubated with 40 μM dynasore before incubating with or without 80 nM human NE for 1 h prior to addition of probe **NEP**. All the above pre-treated cells were incubated with probe **NEP** (1 μM) for 30 min and Hoechst 33342 (10 μM) for 5 min at 37 °C, and the fluorescence images were acquired with an inverted fluorescence microscope (Olympus IX71, Japan). The fluorescence image data were analyzed by quantifying the fluorescence intensity of **NEP** in each cell using Image J software (National Institutes of Health, America). Each experiment was performed in three independent biological replicates.

Live imaging in ALI model mice. Wild type C57 mice and nude mice were purchased from Huafukang Bioscience Co., Ltd. (Beijing, China). Mice were intravenous injected with or without 5 mg/kg LPS and further kept for 48 h. After barbered and intravenous injected with 200 μL **NEP** (50 μM) for 30 min, all the mice were imaged with IVIS Lumina XRMS III *in vivo* imaging system (PerkinElmer, USA).

RESULTS AND DISCUSSIONS

Probe design and characterization

In our previously work, we reported the discovery of a pentafluoroethyl conjugated 7-amino-4-trifluomethylcoumarin as the first non-peptide fluorescent substrate for human NE.[24] Unfortunately, the specificity and the green fluorescence of the fluorophore restricted its further application in cells and animal model. To obtain a specific NE probe with improved properties for real-time monitoring and visualizing

human NE in living cells and animals, we designed a new near-infrared probe with a hemicyanine based fluorophore which already showed its excellent performance in biological samples and living system.[22, 25] Thus, we further synthesized this probe and the detail is described in the experimental section, the chemical structure is also fully verified (Figures S1-S5). As expected, the intact **NEP** is well quenched, and generated strong red fluorescence upon the addition of human NE.

We firstly studied the effects of pH and the temperature for **NEP** characterization at aqueous solution. It was found that the optimum pH and temperature are around pH = 7.0 and 37 ℃, respectively, which are very close to physical environment (Figures S6 and S7). Under the optimized conditions, we examined the time-dependent fluorescence spectra of the **NEP** when incubating with appropriate amount of human NE (Figure 1a). Similarly, we also tested the human NE dose-dependent enhancement of the fluorescence intensity of **NEP** at the maximum emission wavelength of 700 nm (Figure 1b). Interestingly, the hydrolysis of **NEP** catalyzed by human NE was very fast, and the fluorescence intensity (λ_{em}max = 700 nm) reached the maximum value within 20 min and the enhancement is about 25-fold comparing to the basal level. In addition, the fluorescence response of **NEP** vs the different concentrations of human NE (0-1.0 μg/mL) was in a good linearity from which the limit of detection (LOD) was determined to be 29.42 ng/mL (Figure 1c). Moreover, the specificity of **NEP** was also investigated against various analytes. Considering the previous report that a rhodamine probe containing trifluoroacetamide can be hydrolyzed by PLE[26], we screened some common used esterases or amidases in aqueous buffer solution to figure out the specificity of **NEP**. As anticipated, **NEP** shows very high specificity for human NE, since the responses caused by other amidases (chymotrypsin, trypsin, carboxypeptidase A, carboxypeptidase B) were negligible (Figure 1d). Although PLE did show weak response toward **NEP**, the two major human sources of liver esterase (BChE and carboxylesterase) displayed almost no interference against NE detection with **NEP**. Meanwhile, no significant interference by amino acids and metal anions was observed for sensing human NE with NEP (Figure S8). To explain why the use of the hemicyanine based fluorophore is more sensitive and selective for NE compared

to the aminocoumarin based fluorophore[24], molecule docking was carried out to get their stimulated binding modes in the active site of HNE, respectively (Figure S9). It revealed that **NEP** shows a closer distance between its amide bond and the key catalytic residue Ser195, suggesting that **NEP** could be more prone to be attacked by Ser195. This data taking together indicates that **NEP** can be a useful tool for NE profiling in rather complicated biological environments.

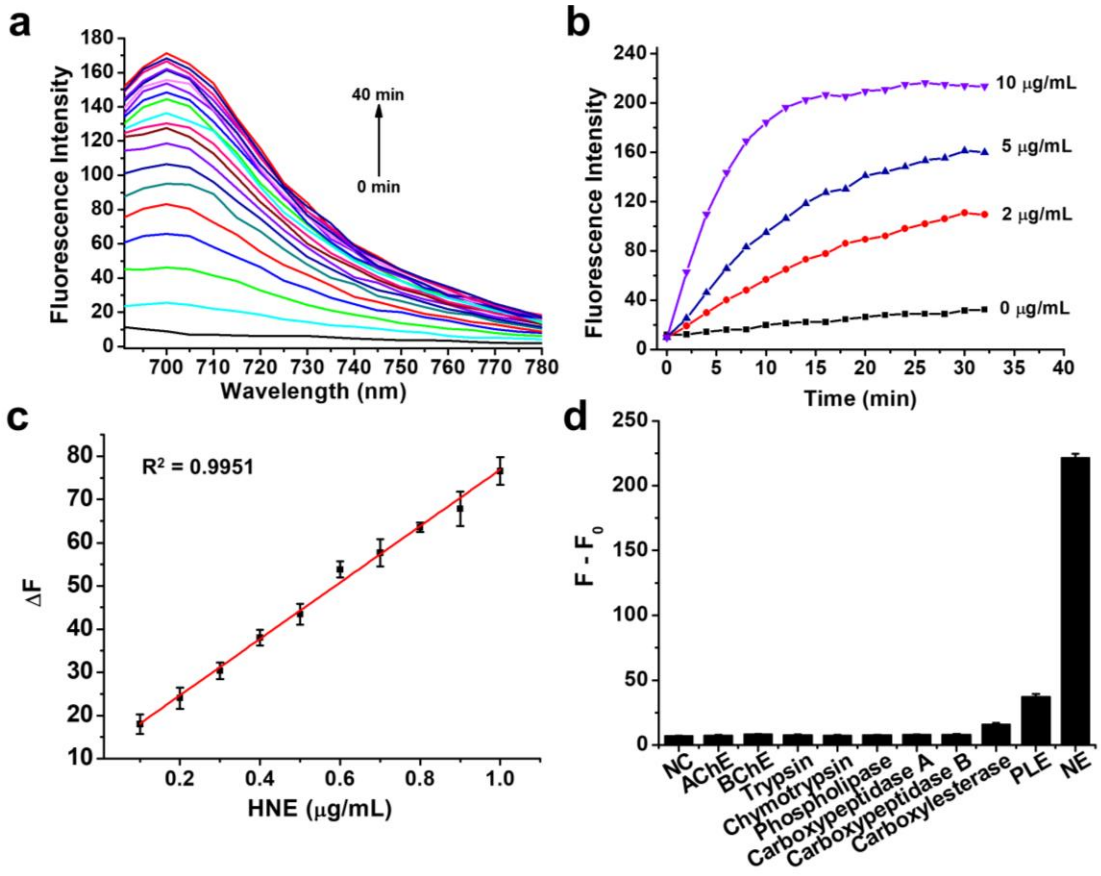

Figure 1. Kinetic characterization of **NEP** as a fluorogenic substrate for human NE. (a) Time-dependent fluorescent spectrum of **NEP** after the addition of 10 μg/mL human NE. (b) Fluorescence intensity (λ_{em}max = 700 nm) of **NEP** when incubating with various concentration of (0, 2, 5, 10 μg) human NE. (c) Linearity curve of fluorescence intensity vs the concentration of human NE ranging from 0 to 1 μg/mL. (d) Fluorescence responses of **NEP** (10 μM) against different hydrolases (10 μg/mL). AChE refers to acetylcholinesterase, BChE refers to butyrylcholinesterase and PLE represents to porcine liver esterase.

Visualization of NE trafficking in living cells.

As is well known, NE is specifically expressed in immune cells that are usually suspended in growth medium, which is unfavorable for live imaging. We hence chose a chemical-treated adherent growth leukemia cell line RBL-2H3[27] as the model for living cell image. Prior to the cell imaging studies, we tested the cytotoxicity of **NEP** by MTT assay and observed no apparently toxicity against RBL-2H3 cells at various concentrations for 24 h (Figure S10). As shown in Figure 2a, the incubation with **NEP** and the routine nuclear staining with Hoechst 33342 for 30 min led to the robust red and blue fluorescent response in cells, respectively. It is worth to mention that some strong red fluorescent puncta were observed, and we initially thought it might be localized in cell membrane because the localization of active form of endogenous NE is in cell membrane.[27] However, we co-stained the cells with **NEP** and the commercial cell membraned dye D4292, and found that the signal was not localized in cell membrane (Figure S10). Considering the cation containing fluorophore of **NEP**, we speculated that the free fluorophore might gather into the mitochondria. Thus, we further stained the cells with **NEP** and commercial dye mito-tracker green together, and found that the they were highly colocalized (Figure S11), indicating that signal of **NEP** is eventually gathered in mitochondria. Two common NE inhibitors, DHPI and the commercial drug sivelestat, were pre-incubated with cells prior to the addition of **NEP.** Consequently, the red fluorescence intensity significantly declined around 50% comparing to the DMSO-treated control group (Figure 2b). More importantly, the fluorescence signal in cell membrane was almost eliminated after the pre-incubation with sivelestat, which further indicated that the fluorescent signal was attributed to the NE activity.

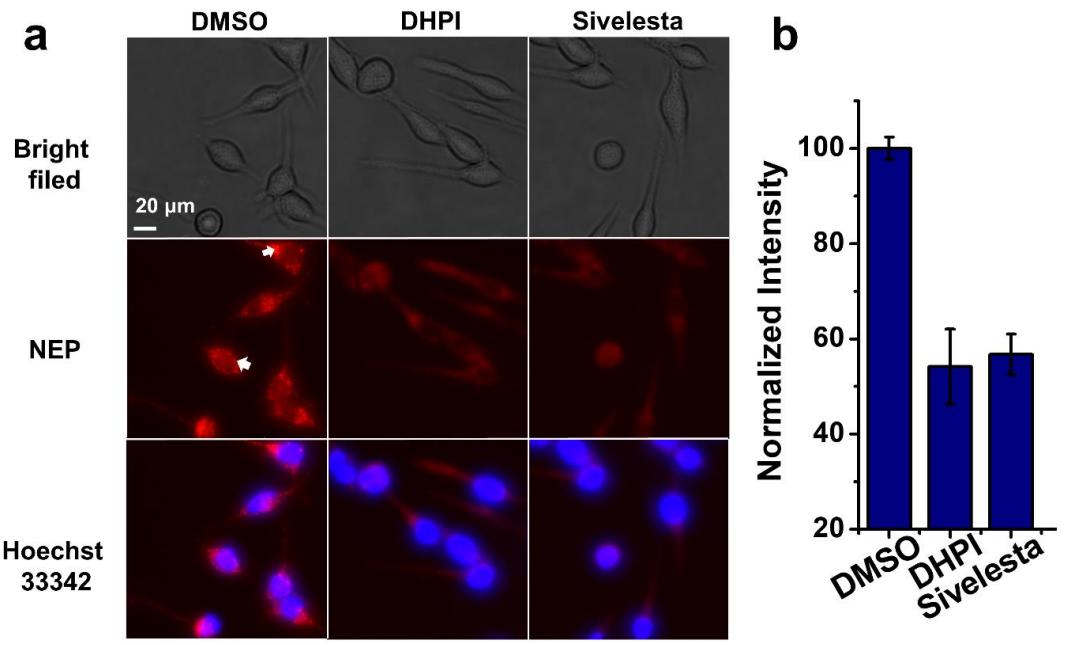

Figure 2. Live image with **NEP** in RBL-2H3 cells. (a) Fluorescence images of RBL-2H3 cells pre-treated with or without NE inhibitors for 3 h before incubation with 1 μM **NEP** for 30 min. (b) Analysis of relative FI shown in left panel. (**P < 0.01, data analyses were performed with an independent samples t-test with equal variances, means ± s.d., n = 3 independent experiments. λ_{ex} = 590-650 nm, λ_{em} = 660-730 nm.)

To investigate the probability of demonstrating subcellular trafficking of active NE by **NEP**, brefeldin A (BFA), an inhibitor that can arrest protein transport to Golgi and redistribution to endoplasmic reticulum (ER)[27] was applied in this study. As depicted in Figure 3a, the fluorescence is mainly distributed outer cellular when the cells were treated with **NEP** (Figure 3a). However, upon the stimulation with BFA for 16 h, the fluorescent signal appeared to be constitutively internalized, which suggested that the transport of matured NE to cell membrane was blocked by BFA (Figure 3b). Moreover, after removing of BFA and further incubated the cells for 30 min, the internalization of **NEP** signal was relieved (Figure 3c), indicating the transportation of intracellular NE was recovered. Intriguingly, in the control experiment with the fluorophore **HCY-NH$_2$** (Figure S12), the fluorescent signal was freely scattered throughout the cells and no matter treated with or without BFA.

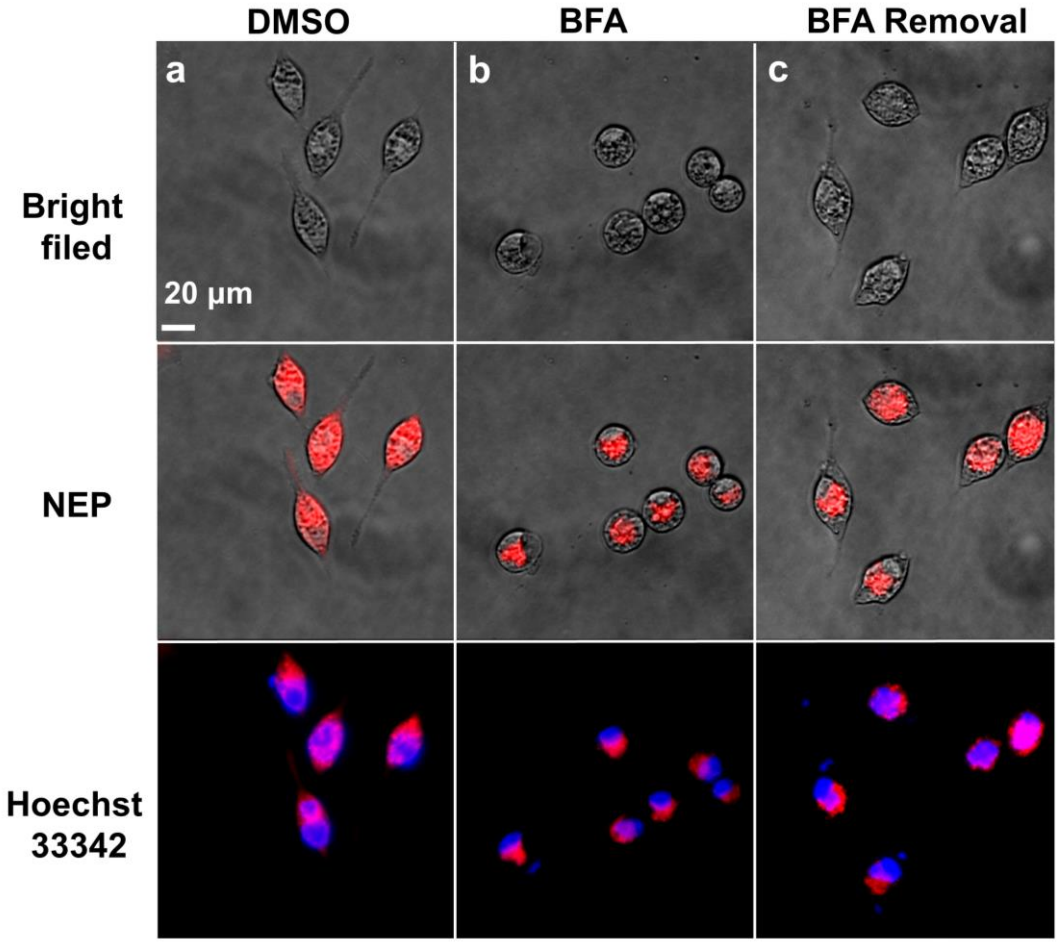

Figure 3. Monitoring NE trafficking in RBL-2H3 cells with **NEP**. (a-b) RBL-2H3 cells pre-treated with 0.5% DMSO or 2 μM BFA for 16 h before incubation with 1 μM **NEP** for 30 min. (c) RBL-2H3 cells pre-treated with 2 μM BFA for 16 h and then removal of BFA for 30 min before incubation with 1 μM **NEP** for 30 min. (λ_{ex} = 590-650 nm, λ_{em} = 660-730 nm.)

With the help of immunofluorescence assay, a decisive study concerning the association of NE with lung cancer claimed that exogenous NE could be uptaken into cancer cells and the growth was promoted accordingly.[14] To further in situ image the process of NE uptaking, **NEP** was applied to visualize A549 cells stimulated with exogenous NE. As shown in Figure 4a, pre-incubated with 80 nM human **NE** resulted in robust and punctate fluorescence in single cell imaging, while the background fluorescence in control group treated with only DMSO was very negligible. To obtain

plausible evidence, we also employed dynasore, a dynamin inhibitor to block the cell permeability by inhibiting clathrin-mediated endocytosis[28] before the subsequent treatment with external human NE and probe **NEP**. Intriguingly, the fluorescence intensity of the A549 cells pre-incubated with dynasore indeed become weaker than that of cells only treated with human NE and probe **NEP**. Besides, we also applied **NEP** to study the uptake of NE in MDA-MB-231 cells with same method described in the literature,[29] and obtained the similar result (Figure S13). The above observations lead us to conclude that, **NEP** is a reliable and specific tool to visualize NE trafficking and up-taking processes.

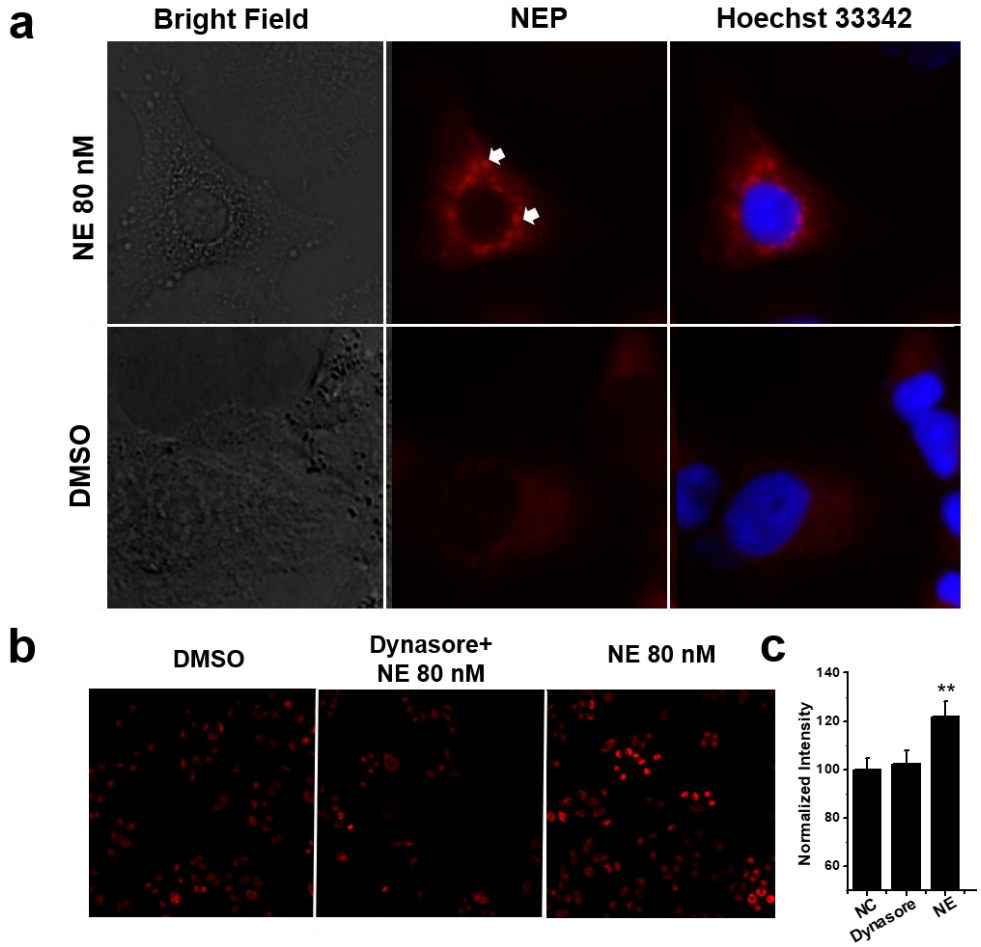

Figure 4. Monitoring of NE-uptake in A549 cells by **NEP**. (a) Fluorescent image with A549 cells pre-incubated with or without 80 nM human NE for 1h before incubated with 1 μM **NEP** for 30 min. (b) Fluorescent image taken from A549 pre-incubated with or without 40 μM dynasore for 1h before incubated with 80 nM human NE for 1h. (c) Analysis of relative FI shown in panel b. (**P < 0.01, data

analyses were performed with an independent samples t-test with equal variances, means ± s.d., n = 3 independent experiments. λ_{ex} = 590-650 nm, λ_{em} = 660-730 nm.)

To evaluate the performance of **NEP** in the context of lung diseases related mechanism study, we imaged and quantitatively analyzed the regulation of endogenous NE activity in cells in the presence of stimulating factors. As mentioned before, NE plays important role in immune system and elevated in inflammatory response. LPS is a typical macromolecule that can induce inflammation in cells and animals,[30] and two pro-inflammation factors IL-6 and TNF-α,[31-32] are common reagents to induce inflammatory response. As displayed in Figure 5, pronounced increases of the red fluorescence in cells separately treated with LPS, IL-6 and TNF-α. After quantifying the fluorescence intensities for each group of cells, all the pre-treated cells showed over 50% elevation when compared with DMSO-treated control. This data suggests that the up-regulation of NE triggered by stimulation factors can be directly visualized with **NEP** at the cellular level.

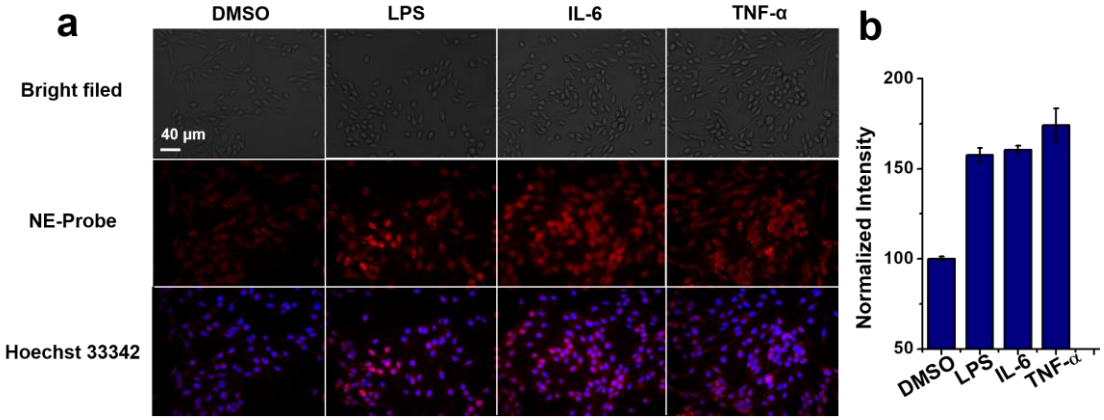

Figure 5. Up-regulation of NE in RBL-2H3 cells induced by LPS and pro-inflammation factors. (a) Fluorescence images of RBL-2H3 cells pre-treated with DMSO (0.5%), LPS (20 μg/mL), IL-6 (100ng/mL) and TNF-α (100ng/mL) before incubation with 1μM **NEP** for 30 min. (b) Analysis of relative fluorescence intensity shown in left panel. (**P < 0.01, data analyses were performed with an independent samples t-test with equal variances, means ± s.d., n = 3 independent experiments. λ_{ex} = 590-650 nm, λ_{em} = 660-730 nm.)

***In vivo* imaging of NE in ALI model mice.**

Human NE is a major cause for acute lung injury (ALI) due to its elevated proteolytic activity that destroy the normal lung tissue.[6-7] However, the detailed response of lungs to ALI remains unclear. Fluorescent probes are attractive to tracking the desired enzyme level *in vivo*, but no small-molecular fluorogenic probe are available for NE imaging in live animals. Thus, **NEP** was applied in the constructed ALI model mice generated by LPS injection. In general, healthy mice and ALI model mice were intravenous injected with 200 μL **NEP** (50 μM) for 30 min before gas anesthesia and fluorescence image. To our delight, very low fluorescent signal was detected in control group mice (left in Figure 6a), whereas remarkable fluorescent signal is acquired in ALI model mice group (right in Figure 6a). However, the signal were observed in the abdomen of the mice instead of the chest. To understand this phenomenon, we further investigated the distribution of **NEP** signal in ALI nude mice model. As shown in Figure S14, the fluorescent signal in ALI nude mouse was emerged only after 5 min, quickly enhanced within 10 min, suggesting that the **NEP** hydrolysis catalyzed by NE is quite fast. Based on our understanding, there may be two reasons behind this observation: a) the NEP doesn't possess preference toward lung, and could accumulate in multiple organs. Thus the signal is occurred in both lung and other organs; b) the free fluorophore released after the NE catalysis can be quickly metabolized by liver, kidney or intestine. Anyhow, the significantly enhanced fluorescent signal in both ALI model C57 mice and nude mice provides solid evidence that NE was highly elevated in *in vivo* ALI model. We further collected the two most widely used biological samples, bronchoalveolar lavage fluid (BAL) and serum[6, 30] from both healthy control and ALI model mice, and utilized **NEP** to examine the relative contents of NE (Figures. 6b and 6c). No surprise that the NE activity in the biological samples of ALI group is much higher than those of control group, which are in good consistent with the result of the live mouse imaging. To avoid false results, the commercial NE inhibitor, sivelestat, was set to be a positive control group for NE detection in BAL and mice serum. As anticipated, no obvious

fluorescent signal could be detected when the samples were pre-incubated with 10 μM of sivelestat for 10 min. Taking together, our results suggest that **NEP** may serve as a valuable tool for clinical diagnosis of ALI and other NE related disease.

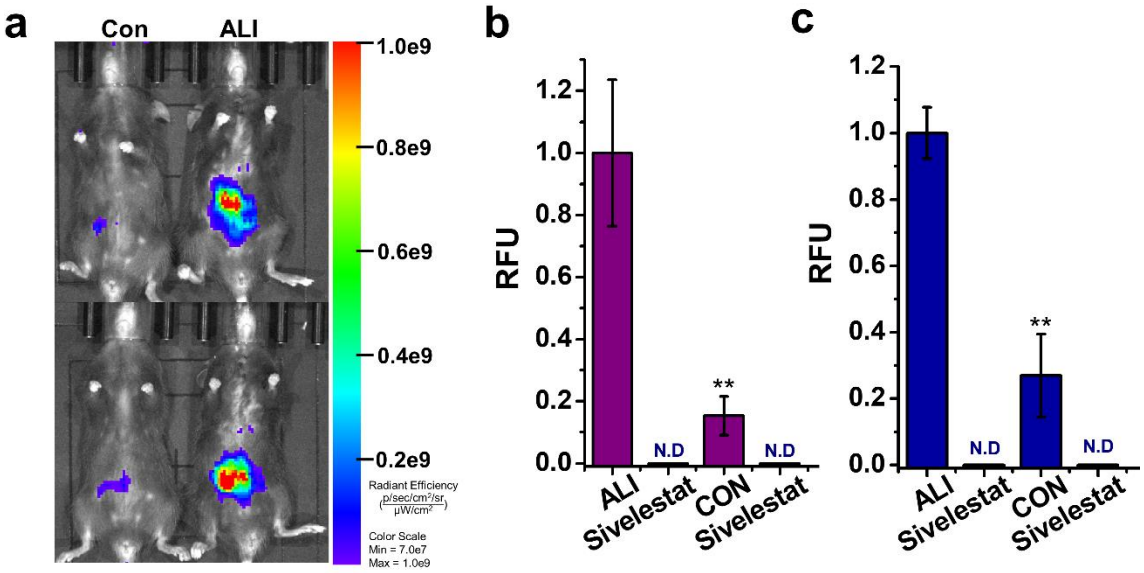

Figure 6. *In vivo* imaging of **NEP** in ALI mice model. (a) Live image of control mice (left) and ALI mice (right) intravenously injected with 200 μL 50 μM **NEP**. (b) Measure of NE activity in BAL from control and ALI mice with **NEP** with or without pre-incubated with 10 μM of sivelestat for 10 min. (c) Measure of NE activity in serum from control and ALI mice with 10 μM **NEP** with or without pre-incubation with 10 μM of sivelestat for 10 min. (**$P < 0.01$, data analyses were performed with an independent samples t-test with equal variances, means ± s.d., n = 3 independent experiments. λ_{ex} = 660 nm, λ_{em} = 670-730 nm.)

CONCLUSION

In summary, we reported a near-infrared fluorescent probe (**NEP**) based on hemicyanine dye for the highly specific detection of human NE *in vitro* and *in vivo*. With this new off-on fluorescent reporter, we have the convenient and fast tool other than complicated and time-consuming immunofluorescence assay, to timely and spatially analyze several important cellular events, such as NE trafficking, NE up taking and LPS induced NE up-regulation. Moreover, we further applied **NEP** in ALI

model mice and demonstrated the capability for quantitative analysis of NE in living mice and biological samples. As far as we know, **NEP** is the first small molecular near-infrared fluorescent probe to detect exogenous and endogenous NE in cells and living organisms. Therefore, it is envisioned that **NEP** may serve as a potential tool for diagnosis and pathological mechanism study of NE-related disease.

ACKNOWLEDGMENT

This work was funded by the National Key Research and Development Program of China (No. 2017YFA0505200) and National Natural Science Foundation of China (No. 21332004, and 21672079); Hubei Province Natural Science Foundation (No. 2018CFA072); the self-determined research funds of Central China Normal University (CCNU18ZDPY01 and CCNU18TS007) from the colleges' basic research and operation of MOE".

SUPPORTING INFORMATION

Organic synthesize, characterization figures and cell imaging experiments are provided in the supporting information. This material is available free of charge via the Internet.

REFERENCES

1. Mantovani, A.; Cassatella, M. A.; Costantini, C.; Jaillon, S., Neutrophils in the activation and regulation of innate and adaptive immunity. *Nat Rev Immunol* **2011,** *11* (8), 519-31.
2. Pham, C. T., Neutrophil serine proteases: specific regulators of inflammation. *Nat Rev Immunol* **2006,** *6* (7), 541-50.
3. M. Gautier., A. J. P. A., S. Janos, H. William, B. Erika Neutrophil Elastase as a Target in Lung Cancer. *Anti-Cancer Agents in Medicinal Chemistry* **2012,** *12*, 565-579.
4. Korkmaz, B.; Moreau, T.; Gauthier, F., Neutrophil elastase, proteinase 3 and

cathepsin G: Physicochemical properties, activity and physiopathological functions. *Biochimie* **2008,** *90* (2), 227-242.

5. Owen, C. A., Roles for proteinases in the pathogenesis of chronic obstructive pulmonary disease. *Int J Chron Obstruct Pulmon Dis* **2008,** *3*, 253-268.
6. Tao, W.; Miao, Q. B.; Zhu, Y. B.; Shu, Y. S., Inhaled neutrophil elastase inhibitor reduces oleic acid-induced acute lung injury in rats. *Pulm Pharmacol Ther* **2012,** *25* (1), 99-103.
7. Ishii, T.; Doi, K.; Okamoto, K.; Imamura, M.; Dohi, M.; Yamamoto, K.; Fujita, T.; Noiri, E., Neutrophil elastase contributes to acute lung injury induced by bilateral nephrectomy. *Am J Pathol* **2010,** *177* (4), 1665-73.
8. Taggart, C. C.; Greene, C. M.; Carroll, T. P.; O'Neill, S. J.; McElvaney, N. G., Elastolytic proteases: inflammation resolution and dysregulation in chronic infective lung disease. *Am J Respir Crit Care Med* **2005,** *171* (10), 1070-6.
9. Fujii, M.; Miyagi, Y.; Bessho, R.; Nitta, T.; Ochi, M.; Shimizu, K., Effect of a neutrophil elastase inhibitor on acute lung injury after cardiopulmonary bypass. *Interact Cardiovasc Thorac Surg* **2010,** *10* (6), 859-62.
10. Miyoshi, S.; Hamada, H.; Ito, R.; Katayama, H.; Irifune, K.; Suwaki, T.; Nakanishi, N.; Kanematsu, T.; Dote, K.; Aibiki, M.; Okura, T.; Higaki, J., Usefulness of a selective neutrophil elastase inhibitor, sivelestat, in acute lung injury patients with sepsis. *Drug Des Devel Ther* **2013,** *7*, 305-16.
11. Iwata, K.; Doi, A.; Ohji, G.; Oka, H.; Oba, Y.; Takimoto, K.; Igarashi, W.; Gremillion, D. H.; Shimada, T., Effect of Neutrophil Elastase Inhibitor (Sivelestat Sodium) in the Treatment of Acute Lung Injury (ALI) and Acute Respiratory Distress Syndrome (ARDS): A Systematic Review and Meta-Analysis. *Internal Medicine* **2010,** *49* (22), 2423-2432.
12. Kuna, P.; Jenkins, M.; O'Brien, C. D.; Fahy, W. A., AZD9668, a neutrophil elastase inhibitor, plus ongoing budesonide/formoterol in patients with COPD. *Respir Med* **2012,** *106* (4), 531-9.
13. Wilson, D. O.; Weissfeld, J. L.; Fuhrman, C. R.; Fisher, S. N.; Balogh, P.; Landreneau, R. J.; Luketich, J. D.; Siegfried, J. M., The Pittsburgh Lung

Screening Study (PLuSS): outcomes within 3 years of a first computed tomography scan. *Am J Respir Crit Care Med* **2008,** *178* (9), 956-61.

14. Houghton, A. M.; Rzymkiewicz, D. M.; Ji, H.; Gregory, A. D.; Egea, E. E.; Metz, H. E.; Stolz, D. B.; Land, S. R.; Marconcini, L. A.; Kliment, C. R.; Jenkins, K. M.; Beaulieu, K. A.; Mouded, M.; Frank, S. J.; Wong, K. K.; Shapiro, S. D., Neutrophil elastase-mediated degradation of IRS-1 accelerates lung tumor growth. *Nat Med* **2010,** *16* (2), 219-23.
15. Talukdar, S.; Oh, D. Y.; Bandyopadhyay, G.; Li, D.; Xu, J.; McNelis, J.; Lu, M.; Li, P.; Yan, Q.; Zhu, Y.; Ofrecio, J.; Lin, M.; Brenner, M. B.; Olefsky, J. M., Neutrophils mediate insulin resistance in mice fed a high-fat diet through secreted elastase. *Nat Med* **2012,** *18* (9), 1407-12.
16. Liu, H. W.; Li, K.; Hu, X. X.; Zhu, L.; Rong, Q.; Liu, Y.; Zhang, X. B.; Hasserodt, J.; Qu, F. L.; Tan, W., In Situ Localization of Enzyme Activity in Live Cells by a Molecular Probe Releasing a Precipitating Fluorochrome. *Angew Chem Int Ed Engl* **2017,** *56* (39), 11788-11792.
17. Asanuma, D.; Sakabe, M.; Kamiya, M.; Yamamoto, K.; Hiratake, J.; Ogawa, M.; Kosaka, N.; Choyke, P. L.; Nagano, T.; Kobayashi, H.; Urano, Y., Sensitive beta-galactosidase-targeting fluorescence probe for visualizing small peritoneal metastatic tumours in vivo. *Nat Commun* **2015,** *6*, 6463.
18. Park, S. J.; Lee, H. W.; Kim, H.-R.; Kang, C.; Kim, H. M., A carboxylesterase-selective ratiometric fluorescent two-photon probe and its application to hepatocytes and liver tissues. *Chemical Science* **2016,** *7* (6), 3703-3709.
19. Kathayat, R. S.; Elvira, P. D.; Dickinson, B. C., A fluorescent probe for cysteine depalmitoylation reveals dynamic APT signaling. *Nat Chem Biol* **2017,** *13* (2), 150-152.
20. Hirayama, S.; Hori, Y.; Benedek, Z.; Suzuki, T.; Kikuchi, K., Fluorogenic probes reveal a role of GLUT4 N-glycosylation in intracellular trafficking. *Nat Chem Biol* **2016,** *12* (10), 853-9.
21. Li, L.; Zhang, C. W.; Chen, G. Y.; Zhu, B.; Chai, C.; Xu, Q. H.; Tan, E. K.; Zhu,

Q.; Lim, K. L.; Yao, S. Q., A sensitive two-photon probe to selectively detect monoamine oxidase B activity in Parkinson's disease models. *Nat Commun* **2014,** *5*, 3276.

22. He, X.; Li, L.; Fang, Y.; Shi, W.; Li, X.; Ma, H., In vivo imaging of leucine aminopeptidase activity in drug-induced liver injury and liver cancer via a near-infrared fluorescent probe. *Chem Sci* **2017,** *8* (5), 3479-3483.
23. Xie, X.; Yang, X.; Wu, T.; Li, Y.; Li, M.; Tan, Q.; Wang, X.; Tang, B., Rational Design of an alpha-Ketoamide-Based Near-Infrared Fluorescent Probe Specific for Hydrogen Peroxide in Living Systems. *Anal Chem* **2016,** *88* (16), 8019-25.
24. Sun, Q.; Li, J.; Liu, W. N.; Dong, Q. J.; Yang, W. C.; Yang, G. F., Non-peptide-based fluorogenic small-molecule probe for elastase. *Anal Chem* **2013,** *85* (23), 11304-11.
25. He, X.; Hu, Y.; Shi, W.; Li, X.; Ma, H., Design, synthesis and application of a near-infrared fluorescent probe for in vivo imaging of aminopeptidase N. *Chem Commun (Camb)* **2017,** *53* (68), 9438-9441.
26. Abney, K. K.; Ramos-Hunter, S. J.; Romaine, I. M.; Goodwin, J. S.; Sulikowski, G. A.; Weaver, C. D., Selective Activation of N,N'-Diacyl Rhodamine Pro-fluorophores Paired with Releasing Enzyme, Porcine Liver Esterase (PLE). *Chemistry* **2018,** *24* (36), 8985-8988.
27. Tapper, H.; Källquist, L.; Johnsson, E.; Persson, A.-M.; Hansson, M.; Olsson, I., Neutrophil elastase sorting involves plasma membrane trafficking requiring the C-terminal propeptide. *Experimental Cell Research* **2006,** *312* (18), 3471-3484.
28. Macia, E.; Ehrlich, M.; Massol, R.; Boucrot, E.; Brunner, C.; Kirchhausen, T., Dynasore, a cell-permeable inhibitor of dynamin. *Dev Cell* **2006,** *10* (6), 839-50.
29. Kerros, C.; Tripathi, S. C.; Zha, D.; Mehrens, J. M.; Sergeeva, A.; Philips, A. V.; Qiao, N.; Peters, H. L.; Katayama, H.; Sukhumalchandra, P.; Ruisaard, K. E.; Perakis, A. A.; St John, L. S.; Lu, S.; Mittendorf, E. A.; Clise-Dwyer, K.; Herrmann, A. C.; Alatrash, G.; Toniatti, C.; Hanash, S. M.; Ma, Q.; Molldrem, J. J., Neuropilin-1 mediates neutrophil elastase uptake and cross-presentation in breast cancer cells. *J Biol Chem* **2017,** *292* (24), 10295-10305.

30. Vlahos, R.; Wark, P. A.; Anderson, G. P.; Bozinovski, S., Glucocorticosteroids differentially regulate MMP-9 and neutrophil elastase in COPD. *PLoS One* **2012,** *7* (3), e33277.
31. Zimmermann, P.; Ziesenitz, V. C.; Curtis, N.; Ritz, N., The Immunomodulatory Effects of Macrolides-A Systematic Review of the Underlying Mechanisms. *Front Immunol* **2018,** *9*, 302.
32. Barnes, P. J., The cytokine network in asthma and chronic obstructive pulmonary disease. *J Clin Invest* **2008,** *118* (11), 3546-56.

For TOC only

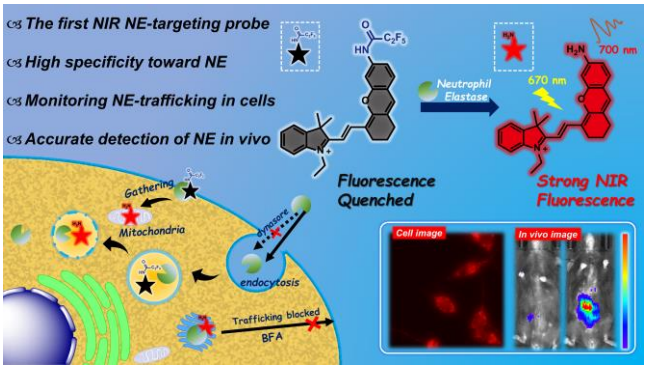
The first NIR NE-targeting probe
High specificity toward NE
Monitoring NE-trafficking in cells
Accurate detection of NE in vivo
Neutrophil Elastase
670 nm
700 nm
Fluorescence Quenched
Strong NIR Fluorescence
Gathering
Mitochondria
endocytosis
Trafficking blocked
BFA
Cell image
In vivo image